Journal of Physics: Conference Series

PAPER • OPEN ACCESS

Biochar powders coating to improve evaporative cooling in Maisotsenko-cycle systems

To cite this article: N Morselli *et al* 2024 *J. Phys.: Conf. Ser.* **2685** 012067

View the article online for updates and enhancements.

You may also like

- Fluid dynamic parameters of naturally derived hydroxyapatite scaffolds for *in vitro* studies of bone cells
E Salerno, A d'Adamo, G Corda et al.
- Lightweight solution for existing steel movable bridge retrofit and repair
Antonella Ruzzante and Roberto Pavan
- Assessment of existing steel bridges: codes and standard
Erica Siviero and Roberto Pavan

This content was downloaded from IP address 155.185.226.77 on 11/06/2024 at 08:52

Biochar powders coating to improve evaporative cooling in Maisotsenko-cycle systems

N Morselli[1,*], F D Fracasso[1], M Cossu[1], F Ottani[1], M Puglia[1], S Pedrazzi[1], G Allesina[1], A Muscio[1] and P Tartarini[1,2]

[1] Department of Engineering "Enzo Ferrari", University of Modena and Reggio Emilia, Via Vivarelli 10/1 – 41125 Modena, Italy

.

[2] INTERMECH—Inter-Departmental Center, University of Modena and Reggio Emilia, Via Vivarelli 2 – 41125 Modena, Italy.

[*] Corresponding author: nicolo.morselli@unimore.it

Abstract. This work presents an experimental study on the performance of biochar powder coatings on aluminum surfaces for use in indirect evaporative coolers based on the Maisotsenko cycle. The performance of the biochar coated samples was compared to cellulose-coated aluminum samples and uncoated ones. Results showed that biochar coatings improved the performance of uncoated aluminum, with the 150 μm particle size coating offering performance comparable to cellulose. However, wetting times were longer, which has implications for spraying strategies.

1. Introduction

A rediscovered alternative to vapor compression systems lays on indirect evaporative cooler based on the Maisotsenko cycle. These systems exploit the latent heat of water evaporation to cool an air flow, thus eliminating the compression work and the need to use refrigerant fluids with positive impact on the environment.

Despite reaching coefficients of performance 5-6 times higher than traditional cooling systems [1], evaporative coolers are often penalized by continuous pump operation for the constant spray of water in the secondary channel in order to obtain a homogeneous humidification of the heat transfer surface [2]. Considerable efforts have been made over the years to improve the water retention and water diffusion of the materials used aiming at reducing the energy consumption for water pumping and further improve the COP.

Several researches focused on the study of porous materials for the wet duct of the heat exchanger, such as: cellulose fiber coating for metal foils, cotton wool, honeycomb structures, coconut fiber, polymer sheets, stainless steel with sintered nickel layer, etc [3, 4].

This work aims to study the water retention and water diffusion capability of biochar powder deposited on aluminum surfaces.

Biochar is a byproduct of the thermochemical process of gasification of wood biomass and is characterized by high porosity and surface area, as well as high resistance over time.

Content from this work may be used under the terms of the Creative Commons Attribution 3.0 licence. Any further distribution of this work must maintain attribution to the author(s) and the title of the work, journal citation and DOI.
Published under licence by IOP Publishing Ltd

Biochar has a particle size that depends on the type of biomass used in the gasification process, ranging from tens of millimetres to a few microns. In this work it was test the performance of biochar coatings with a particle size of less than 250 μm.

Aluminum supports measuring 50x50 mm and with a thickness of 100 μm were specifically made for the deposition of biochar powders. This was achieved by utilizing an epoxy resin layer as an adhesive.

A prototype of evaporative heat exchanger was used to test the specimens. This heat exchanger had the ability to connect to a thermal imaging camera (IR camera), which allowed for the observation of temperature distribution on the lower surface of the specimen.

The analyses of temperature and relative humidity at the inlet and outlet led to the measurement of the temperature drop of the air stream generated by the tested specimen, as well as the water evaporation rate offered by each specimen. Through IR images were gathered data on the homogenization of the water distribution on the coated surface and on the stabilization time of the surface temperature, an index of the diffusion speed of the water on the specimen. Performance of biochar-coated specimens were compared to non-coated and cellulose-coated aluminium specimens.

The next section describes the test methods and the test rig used.

2. Materials and methods

2.1 Maisotsenko's cycle

In the Maisotsenko cycle, ambient air is cooled in a heat exchanger. In the simplest configuration of the cycle, a counter flow heat exchanger can be used (box in Fig. 1).

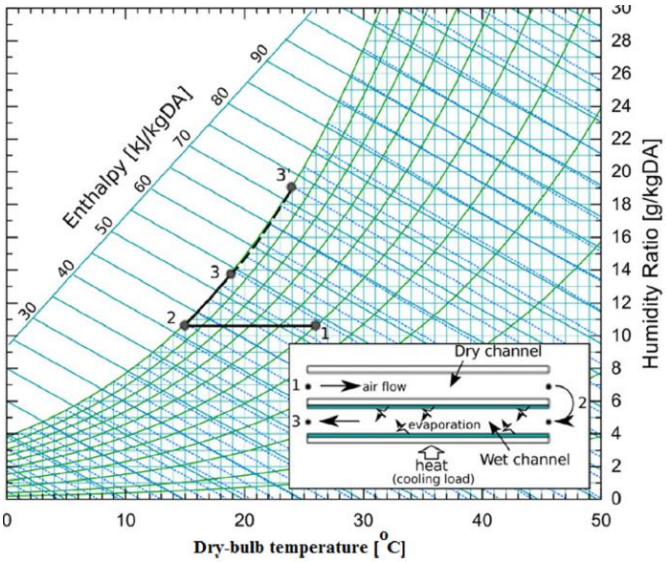

Figure 1. Psychrometric chart and principle of the Maisotsenko cycle: 1) ambient air; 2) released cooled non-humidified air; 3) wet-bulb temperature at ambient conditions; 3') released moist air. (Adapted from Dizaji et al, 2018 [13])

The Maisotsenko cycle involves cooling ambient air in a heat exchanger, typically by using a counter flow heat exchanger with a "dry" duct and a "wet" duct separated by a wall.

Air is introduced into the dry duct, where it is cooled by transferring heat through the separating wall. Some of the cooled air is released as non-humidified air, while the rest is diverted into the wet duct, where it is saturated with liquid water that is continuously vaporized. The air is warmed in the wet duct by heat transferred from the cooled dry air through the separating wall, and it is released into the ambient environment at close to saturation. The Maisotsenko cycle can theoretically cool the non-

humidified air to the dew point temperature, which is lower than the temperature achieved by direct and indirect evaporative cooling systems. This process is illustrated on a psychrometric chart, where 1-2 represents the cooling process in the dry duct, 2 is the release temperature, and 3 is the dew point temperature. The chart also shows the progressive saturation process in the wet duct from 2 to 3', where the moist air is released.

For this cycle, it therefore becomes important to have a heat transfer surface which, on the one hand, guarantees homogeneous water distribution and a high evaporation rate, and on the other, does not add excessive thermal resistance in order to keep the heat flow between the dry and wet ducts high.

2.2 Tested surfaces

The surfaces were prepared using 100 μm thick aluminum foil which was subsequently coated with biochar of different particle sizes.

The biochar used in these tests comes from a downdraft gasification reactor and has an elemental composition shown in Table 1 along with the BET area (porosity indicator).

Table 1. Biochar chemical-physical characterization

C	H	N	O	S	ASH	BET
42.25 $\%_{w/w}$	0.80 $\%_{w/w}$	0.17 $\%_{w/w}$	56.78 $\%_{w/w}$	0.00 $\%_{w/w}$	33.2 $\%_{w/w}$	420 m^2/g

The as received biochar was sieved according to the ISO 3310-1 reference standard and through a RETSCH model AS200 vibrating sieve [5], in order to obtain three different particle sizes: < 75 μm, (75÷150) μm, (150÷250) μm hereinafter referred to as **75 μm**, **150 μm** and **250 μm**. The biochar powder was glued to a 50x50x0.1 mm aluminum support by spreading a layer of low viscosity two-component epoxy resin (175-225 cps at 25°C). SEM images of the three surfaces obtained are shown in Figure 2.

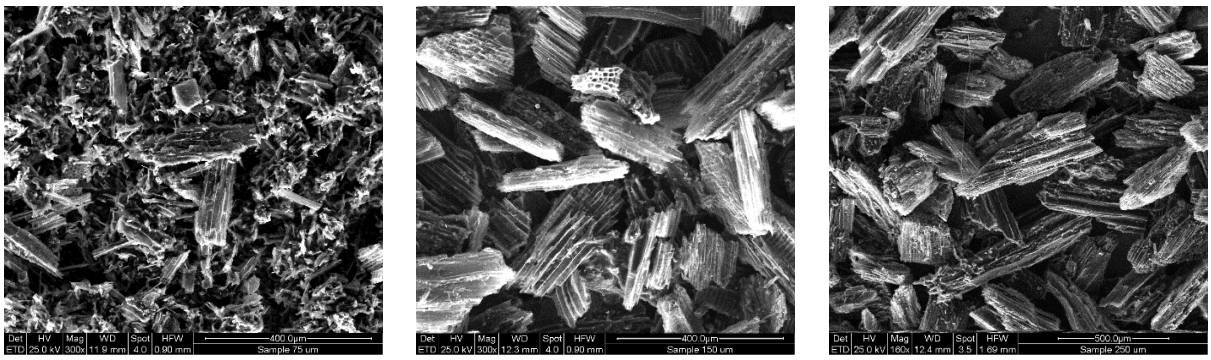

(a) (b) (c)

Figure 2. SEM images of the 75 μm (a), 150 μm (b) and 250 μm (c) biochar coated specimens.

2.3 Experimental setup

The test rig (Figure 3) consists of a rectangular measuring channel delimited at the bottom by the surface to be tested (1) and at the top by a TPU structure (2) which allows the insertion of the micrometric needle (3) used to drip water at controlled flowrate. Each 50x50x0.1 mm surface to be tested is glued to a 3D printed support in order to interface correctly with the test rig (Figure 4). Air with controlled temperature and humidity enters the inlet duct (4) and exits through the outlet duct (5).

The measurement of temperature and humidity is performed in points (6) and (7) through two SHT31 [6] sensors. The lower part of the test rig consists of a closing flange (8) and a housing (9) to insert the IR camera optics which will be directed towards the lower surface of the specimen, painted with matt black. The thermal emissivity of the black surface was measured through the TIR 100-2 emissometer [7] while the IR camera is a FLIR model 640T [8].

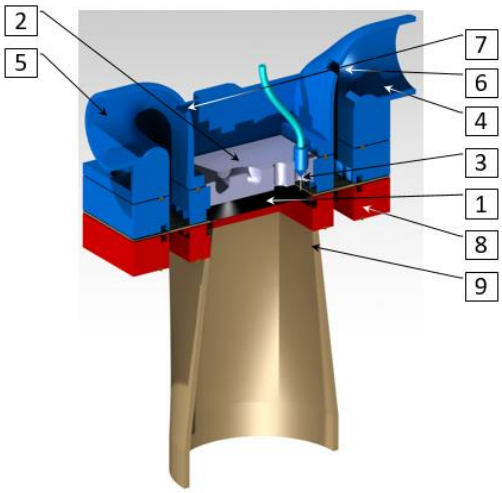

Figure 3. 3D render of the test rig.

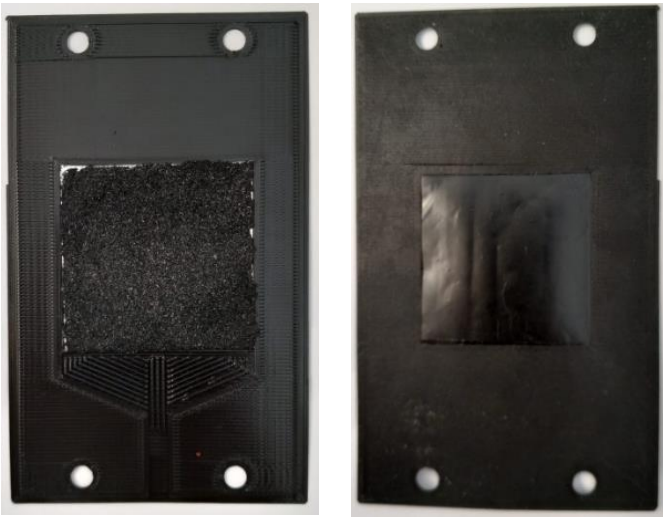

(a) (b)

Figure 4. Front (a) and back (b) of the test specimen support.

2.4 Test methodology

The test methodology adopted aims to reproduce the conditions that occur inside an indirect evaporative heat exchanger. Dry bulb temperature (T_{db}) and inlet air humidity (RH_{in}) were chosen as 40°C and 26.5%RH, respectively. The temperature is controlled through a PTC resistor while the humidity is regulated with an ultrasonic humidifier. The inlet dry air flow ($\dot{m}_{a,dry}$) was chosen equal to 1.44 kg/h in order to have an average air speed in the rectangular duct equal to 1.2 m/s and within the velocity range found in literature that lays between 1 and 2 m/s [9, 10]. Once the test rig reaches steady conditions, the dripper is activated. The inlet and outlet T_{db} and RH are measured through the SHT31 sensors connected to an Arduino UNO board [11], while the temperature of the lower surface of the test specimen (averaged on the entire area of the painted aluminum) is measured through the IR camera software.

Each specimen is subjected to a preheating phase, after which the injection of water is activated at a flow rate ($\dot{m}_{w,in}$) of 3.7 g/h. The water settles on the biochar-coated aluminum specimen and begins to expand while it evaporates. This is followed by an evaporative cooling phase of the air leaving the test channel which continues until it stabilizes at a minimum value. The same happens for the back surface of the specimen, whose average temperature is recorded through the IR camera.

The IR images are used to both assess the uniformity of the water distribution and to measure the surface temperature of the specimen that can be used as comparison between different coatings.

Through the measured data it is possible to calculate the water evaporation rate $\dot{m}_{w,evap}$ as reported in Eq. 1 [12].

$$\dot{m}_{w,evap} = \dot{m}_{a,dry} \cdot (x_{out} - x_{in}) \qquad [\frac{g_{vap}}{h}] \tag{1}$$

Where x_i is the absolute humidity of the moist air calculated according to Eq. 2

$$x_i = 0.622 \cdot \frac{\phi_i \cdot p_{v,sat}}{p_{amb} - \phi_i \cdot p_{v,sat}} \qquad \left[\frac{g_{vap}}{kg_{as}}\right] \tag{2}$$

Where *i* generically represent the *inlet (in)* or *outlet (out)* conditions, ϕ_i is the relative humidity measured through the SHT31 sensors, $p_{v,sat}$ is the water vapor saturation pressure calculated according to the correlation in Eq. 3, calculated at the given air temperature T_i and p_{amb} is the atmospheric pressure considered constant and equal to 101325 Pa.

$$p_{v,sat} = 6.11 \cdot 10^{\frac{7.5 \cdot T_i}{237.2+T_i}} \cdot \phi_i \qquad [Pa] \tag{3}$$

In the following section the results obtained by comparing the different specimens tested are discussed.

3. Results

The plot in Figure 5 shows the time trends of the $\Delta T_{air} = T_{out} - T_{in}$ generated by the evaporation of water on the specimen being tested.

The two benchmarks are represented by the uncoated aluminum specimen (*Al*) and the cellulose coated specimen (*Cellulose*). It can be observed that the *Al* specimen generates the lowest ΔT_{air} while the *Cellulose* specimen presents the most uniform trend among all the samples analysed, reaching a maximum ΔT_{air} equal to 1.4 °C.

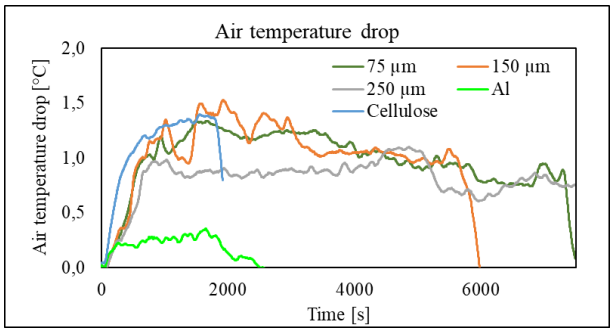

Figure 5. Air temperature drop generated by the different tested specimens.

Although the ΔT_{air} values obtained are comparable to *Cellulose*, less constant trends are observed for biochar-coated samples. The 150 µm coating seems to perform better offering a maximum deltaT equal to 1.5 °C and behaving in a similar way to the 75 µm. The 250 µm instead seems to behave differently in the initial stages, offering a maximum deltaT equal to 1.2 °C. What seems to unite all the biochar coated samples is the slower deltaT rise compared to that obtained with the cellulose sample. This is mainly due to the worse diffusion of water as discussed below.

Figure 6 shows the trends of the water evaporation rate generated by the different samples. The differences in relative humidity that have generated these trends are in the order of 10% and the uncertainty on relative humidity measurement equal to 2% does not lead to strong quantitative assessments. However, the average improvement of the evaporation rate given by the biochar coating compared to the untreated aluminum can be observed. In comparison with *Cellulose*, the biochar offers similar evaporation rates, however generating more discontinuous trends due, as will be seen later, to the partial distribution of water on the surface.

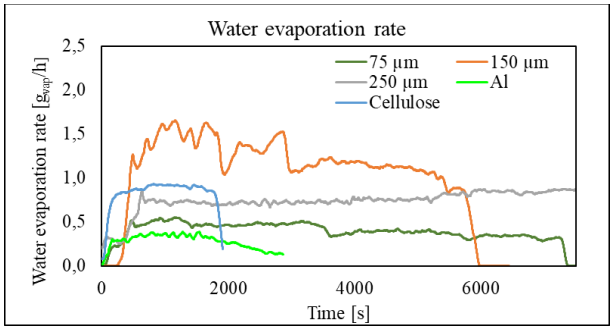

Figure 6. Water evaporation rate generated by the different tested specimens.

The thermographic analyzes returned the temperatures of the lower surface of each sample. Figure 7a shows the temperature of the 75 µm sample at the end of the preheating phase. The sample is heated homogeneously. Figure 7b shows the same sample at the end of the evaporation test: the uneven distribution of water can be seen which tends to create different patterns depending on how the drops descend along the sample. On the other hand, Figure 7c shows the cellulose-coated sample at the end of the same test: the temperature distribution, and consequently the water distribution, is more uniform, which validates the consistent data observed in the previous tests.

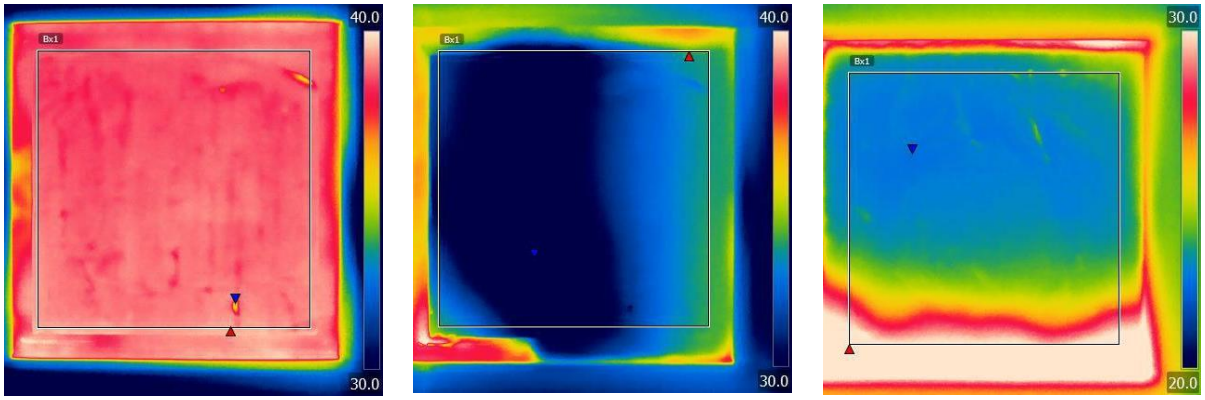

(a) (b) (c)

Figure 7. IR images of the 75 µm specimen at the end of the preheating phase (a), 75 µm (b) and Cellulose (c) at the end of the evaporation test *.

*The temperature scale is $(30-40)°C$ for pictures (a) and (b), while $(20-30)°C$ for (c).

The time required for the surface temperature to stabilize was determined through IR camera recordings. Figure 8 shows the temperature trends of the surfaces by averaging the values over the recording area (45x45 mm due to the presence of the PLA support). For each specimen, the graph was truncated at the point where a stable temperature was reached within a 1% tolerance.

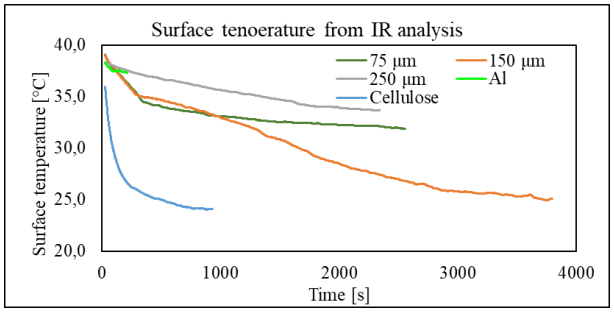

Figure 8. Stabilization time of the surface temperature of the specimens.

Table 2 shows the values of stabilization time and minimum surface temperature for each specimen. The 150 µm specimen reaches a minimum temperature of 24.9 °C, slightly higher than the cellulose specimen, but taking four times longer due to the lower wettability of the biochar-coated surface. The 75 µm specimen has an initial trend similar to the 150 µm specimen, but the minimum temperature is higher at 31.9 °C. The 250 µm specimen reaches a surface temperature of only 33.7 °C. It can be observed that the 150 µm sample achieved a uniform wetting, unlike the 75 µm and 250 µm specimens. Figure 9 shows the IR image of the 150 µm specimen after reaching the stabilization time.

Table 2. IR analysis results

Specimen	Temperature stabilization time [s]	Minmum average surface temperature [°C]
75 µm	2557	33,7
150 µm	3800	24,9
250 µm	2344	33,7
Al	218	36,5
Cellulose	938	24,1

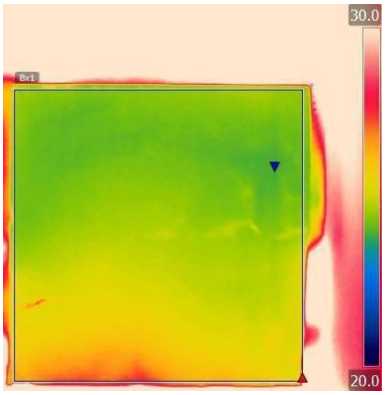

Figure 9. Surface temperature of the specimen 150 µm at the stabilization time.

4. Conclusions

This study experimentally evaluated the performance of aluminum surfaces coated with biochar at different grain sizes, for application in indirect evaporative coolers with particular reference to the Maisotsenko cycle. The biochar coatings always improved the performance of the uncoated aluminum, and in the case of the 150 µm grain size, the performance was comparable to the benchmark identified

in the aluminum specimen coated with cellulose, a material commonly used in evaporative coolers. However, the wetting times were much longer, which has direct implications for spraying strategies.

From the IR analysis, it was observed that the high performance of the 150 μm specimen was enabled by its high wettability, which allowed for a homogeneous diffusion of water and an increased wetted surface area for heat transfer. In the 75 μm and 250 μm specimens, however, the wetting of the sample was only partial.

5. References

[1] Zhu G, Chen W, Lu S 2019. *Chemical Engineering and Processing - Process Intensification*, 145
[2] Ez Abadi A M, Sadi M, Farzaneh-Gord M, Ahmadi M H, Kumar R, & Chau K 2020. *Engineering Applications of Computational Fluid Mechanics*, 14(1), 1-12.
[3] Wani C, Ghodke S, Shrivastava C 2012 *International Journal of Advance Research in Science*, 1(3), 233-237.
[4] Shi W, Min Y, Ma X, Chen Y, Yang H. 2022 *Journal of Building Engineering*, 48, 103898.
[5] RETSCH AS200 datasheet; 2023. Accessed on 2023.04.12
[6] Sensirion SHT31-ARP-B datasheet; 2023Accessed on 2023.04.12
[7] INGLAS GmbH. 2023. TIR 100-2 [Datasheet]. Accessed on 2023.04.12
[8] FLIR. 2023. T640 [Datasheet]. Accessed on 2023.04.12
[9] Riangvilaikul B, Kumar S. 2010. *Energy and Buildings*, 42(5), 637-644.
[10] Duan Z, Zhan C, Zhao X, Dong X. 2016. *Building and Environment*, 104, 47-58.
[11] Arduino. 2023. UNO [Datasheet]. Accessed on 2023.04.12
[12] Çengel YA, Boles MA. 2006. *McGraw-Hill*.
[13] Sadighi Dizaji H, Hu EJ, Chen L, Pourhedayat S. 2018. *Applied Energy*, 228, 2176–2194.

Acknowledgments
N.M. acknowledges the financial support of the FAR Dipartimentale 2023 program of the Dept. of Engineering “Enzo Ferrari” - UniMORE.